though preliminary results in simpler systems are encouraging[25,52] and the iron(II) porphine calculations[21] give good results for other properties.

**Acknowledgment.** We are grateful to the Australian Research Grants Scheme for financial support, the University of Western Australia Crystallography Centre for access to the diffractometer, and Dr. P. E. Fielding for providing the crystals.

(52) Deeth, R. J.; Figgis, B. N.; Ogden, M. I. *Chem. Phys.* **1988**, *121*, 115.

**Registry No.** CoPc, 3317-67-7.

**Supplementary Material Available:** Tables of atomic fractional coordinates, atomic thermal parameters, atomic multipole parameters, least-squares planes, and rigid body translational parameters (8 pages); listing of observed and calculated structure factors corresponding to refinement R3 (25 pages). Ordering information is given on any current masthead page.

# Magnesium Aluminophosphate with Encapsulated Di-*n*-propylamine: Gismondine Structure, Charge-Coupling between Framework Mg and Ammonium Ion, and Molecular Disorder

**Joseph J. Pluth,* Joseph V. Smith, and J. Michael Bennett†**

*Contribution from the Department of the Geophysical Sciences and Materials Research Laboratory, The University of Chicago, Chicago, Illinois 60637, and Union Carbide Molecular Sieves, Tarrytown, New York 10591.* *Received May 9, 1988*

**Abstract:** The crystal structure of the as-synthesized precursor to molecular sieve MAPO-43 was determined by single-crystal X-ray diffraction: $\sim(Al_6Mg_2)P_8O_{32}\cdot 2NC_6H_{16}$, $M_r$ = 1170.7, monoclinic $I112/b$, $a$ = 10.2192 (2) Å, $b$ = 10.2198 (3) Å, $c$ = 10.0126 (3) Å, $\gamma$ = 90.987 (2)°, $V$ = 1045.55 (4) Å$^3$, $Z$ = 1, $D_x$ = 1.897 g cm$^{-3}$, $\lambda$(Cu K$\alpha$) = 1.5418 Å, $\mu$ = 57 cm$^{-1}$, $F(000)$ = 596, $T \sim 295$ K, $R$ = 0.038 for 854 diffractions. A 4-connected framework, with $PO_4$ tetrahedra alternating with $(Al,Mg)O_4$ tetrahedra, has the gismondine topology embracing a 3D channel system bounded by 8 rings. The tetrahedral ordering reduces the symmetry from tetragonal to monoclinic. Two crystallographic types of organic species lie along the channels of each unit cell in a pseudotetragonal array with local order but long-range disorder. To complete the refinement it was necessary to constrain the geometry of the $C_3NC_3$ backbone to a planar zigzag geometry. Each N atom lies close enough to three oxygen atoms of an 8-ring for bifurcated hydrogen bonding; however, the experimental data are too insensitive for direct detection of protons. The chemical and diffraction data are consistent with ionization of the neutral di-*n*-propylamine $HN(C_6H_7)_2$ to an ammonium species $H_2N(C_6H_7)_2$ and associated incorporation of $Mg^{2+}$ into $Al^{3+}$ sites. The combination of charge linkage and molecular disorder implies that the crystallization process from the gel is complex. The key feature in the early stage of the crystallization process might be ionization of each di-*n*-propylamine species and charge linkage to an Mg atom of an $(Mg_xAl_{1-x}P)_n$-oxygen cluster. During crystal growth, all the organic ions have one type of charge linkage to the framework but assume more than one type of offset in the channels.

The physical and chemical properties of a new class of microporous 1:1 aluminophosphates[1,2] are being interpreted in terms of a growing collection of crystal structures.[3,4] These materials were synthesized from aluminophosphate gels with use of a wide range of organic amines and quaternary ammonium cations as structure-directing agents. Aluminum and phosphorus atoms alternate on the vertices of a 4-connected 3D net in each of the new $AlPO_4$ frameworks. Whereas all Al atoms in known aluminosilicate frameworks of as-synthesized zeolites are bonded to only four oxygen atoms, some of the Al atoms in the aluminophosphate frameworks are bonded to one or two extra-framework OH or $H_2O$ species with consequent distortion of the framework. Further geometrical effects result from interaction between the inorganic framework and the encapsulated organic species.

New generations of aluminophosphate-based molecular sieves containing one or more of at least thirteen additional elements in the framework have been synthesized.[5] Those members incorporating a divalent species in a tetrahedral site of the framework are particularly of interest here because an electrostatic charge linkage is indicated with the encapsulated organic species in the as-synthesized material. Furthermore, removal of the encapsulated organic species by calcination may involve formation of a hydroxyl species. Crystal structure and electron probe analysis[6] of the manganese-bearing MnAPO-11 with encapsulated diisopropylamine demonstrated occupancy of one-tenth of the Al sites by Mn. The close approach (2.8 Å) of the N atom of the diisopropylamine species to framework oxygen atoms indicates hydrogen bonding. Addition of $H^+$ to the originally neutral diisopropylamine provides charge balance for the $Mn^{2+}$ incorporation. Hence the structure-directing character of the diisopropylamine in the synthesis of MnAPO-11 from a gel involves an organic–inorganic charge linkage as well as a geometrical template factor.

We now report the crystal structure of a magnesium aluminophosphate synthesized from a gel containing di-*n*-propylamine using conditions similar to those for syntheses of other MAPO materials.[7] Particularly important for the theory of crystallization

* Address correspondence to this author at the University of Chicago.
† Union Carbide Molecular Sieves.

(1) Wilson, S. T.; Lok, B. M.; Messina, C. A.; Cannan, T. R.; Flanigen, E. M. *J. Am. Chem. Soc.* **1982**, *104*, 1146.
(2) Wilson, S. T.; Lok, B. M.; Messina, C. A.; Cannan, T. R.; Flanigen, E. M. *Am. Chem. Soc. Symp. Ser.* **1983**, *218*, 79.
(3) Bennett, J. M.; Dytrych, W. J.; Pluth, J. J.; Richardson, J. W., Jr.; Smith, J. V. *Zeolites* **1986**, *6*, 349.
(4) Bennett, J. M.; Pluth, J. J.; Smith, J. V. *Zeolites*, submitted for publication.
(5) Flanigen, E. M.; Lok, B. M.; Patton, R. L.; Wilson, S. T. *Pure Appl. Chem.* **1986**, *58*, 1351.
(6) Pluth, J. J.; Smith, J. V.; Richardson, J. W., Jr. *J. Phys. Chem.* **1988**, *92*, 2734.
(7) Wilson, S. T.; Flanigen, E. M. U.S. Patent 4567029, January 28, 1986.

0002-7863/89/1511-1692$01.50/0 

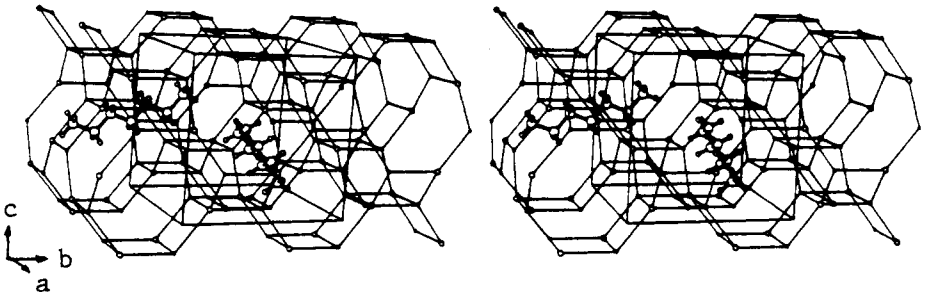


**Figure 1.** Stereoview of the tetrahedral framework of MAPO-43 with two positions for idealized molecules of di-*n*-propylamine. Presence or absence of a circle at the 4-connected nodes distinguishes between positions for Al, Mg, and P. The $C_3NC_3$ backbone of each molecule (large circles) was constrained to be planar. An additional proton was added to the N atom.

for mixed organic–inorganic species is the charge-coupling required between the framework and the encapsulated material and the geometrical disorder of the latter.

## Experimental Section

**Sample Description.** The sample containing MAPO-43 and other aluminophosphate phases was prepared by W. C. Mercer and supplied by S. T. Wilson of Union Carbide Corp. A gel of composition 2.0 *n*-$Pr_2NH$, 0.3 MgO, 0.85 $Al_2O_3$, 1.0 $P_2O_5$, 50 $H_2O$ was heated at 423 K for 222 h. The product was a mixture of MAPO-46, MAPO-43, and MAPO-11. Screening through 325 mesh (40 $\mu$m) increased the concentration of the larger MAPO-43 crystals. Crystals of MAPO-43 appeared to be octahedral in shape, but subsequent X-ray study (Table I, crystallographic data) demonstrated that the symmetry is monoclinic and that the crystal faces comprise {111} and {-111} monoclinic prisms. Weissenberg X-ray photographs showed single sharp diffractions with excellent $\alpha_1$, $\alpha_2$ resolution uncomplicated by twinning.

No chemical analysis was obtained for the multiphase bulk sample. The electron microprobe analysis technique (Cameca SX-50; 15 KV; WDS; standards, $CaAl_2Si_2O_8$ (anorthite glass) for Al, $CaMgSi_2O_6$ (diopside) for Mg, $Ca_2P_2O_7$ for P; PAP data reduction program) was tested on polished crystals of as-synthesized AlPO-5. Oxide totals of 87–88 wt % and a range of 1% about an average value of Al/P = 0.979 were compared with the calculated values of 87.8 wt % oxides and Al/P = 1 for the ideal composition of $Al_{12}P_{12}O_{48}\cdot NC_{12}H_{23}OH$ of this specimen[8] of AlPO-5. Twelve analyses of MAPO-43 crystals in the same specimen mount yielded oxide totals of 77.8–80.5 wt % with MgO 7.4–8.0, $Al_2O_3$ 23.7–26.0, $P_2O_5$ 45.5–47.8. In the absence of evidence of chemical zoning and elemental correlations, the analyses were averaged to MgO 7.6, $Al_2O_3$ 24.8, $P_2O_5$ 46.7 wt %. For full occupancy of metal and oxygen sites in a 4:2-connected three-dimensional framework, and for strict alternation of $(Al_{1-x}Mg_x)$ and P on the 4-connected sites, charge balance could be obtained by Al → Mg + H where the hydrogen is attached either to a framework oxygen or an encapsulated species. The mean electron-microprobe analysis yields an atomic formula $(Al_{0.364}Mg_{0.142}P_{0.494})$ per tetrahedral site. The deviation of 1.3% from an idealized theoretical formula $(Al_{0.36}Mg_{0.14}P_{0.50})$ is within the uncertainty of calibration of electron microprobe analysis. For the 16 tetrahedral sites in the unit cell, this corresponds to $(Al_{5.8}Mg_{2.2}P_8)O_{32}\cdot 2.2H$. If the H species are attached only to the encapsulated di-*n*-propylamine, 2.2 singly ionized molecules should be present in each unit cell. The resulting bulk composition $Al_{5.8}Mg_{2.2}P_8O_{32}\cdot 2.2(H_2NC_6H_{14})$ yields the following oxide values that are within the uncertainty limits of the electron microprobe analysis: MgO 7.42, $Al_2O_3$ 24.75, $P_2O_5$ 47.53 wt %.

**Data Collection.** The selected crystal was coated with oil to control humidity and mounted on a Picker 4-circle diffractometer with the (103) direction 3° from the $\phi$ axis. The small crystal size necessitated the use of a high intensity rotating anode X-ray generator. Refinement using 36 diffractions ($17 < 2\theta < 79°$), each the average of automatic centering of 8 equivalent settings, gave the cell parameters in Table I; the angles are consistent with monoclinic geometry. A total of 1813 intensities yielded 854 unique intensities, all of which were used in refinements; data collection range $h + 11$, $k \pm 11$, $l \pm 11$; maximum intensity variation of 3 standard reflections 3.0%.

The structure was solved using the centric direct methods program in SHELX76.[9] The Al, P, and O atoms were located, included in the model, and refined without difficulty. The Al–O and P–O distances calculated at this point were consistent with alternation of $(Al_{0.72}Mg_{0.28})$ and P atoms on the tetrahedral sites of the framework. This alternation reduces the tetragonal symmetry ($I4_1/amd$) of the neutral framework with idealized geometry (Figure 1) to monoclinic symmetry ($I112/b$). A difference-Fourier synthesis revealed two columns of electron density running parallel to the *a* and *b* axes and staggered along *c* to obey the $4_1$ screw axis of the space group for the neutral framework. It is impossible to account for these columns with a single type of encapsulated molecule, but it was found that overlap from two types of di-*n*-propylamine molecules in different crystallographic positions gave a satisfactory fit. The electron-density section at $x = 0$ (Figure 2a) shows a set of peaks with incomplete resolution. The section at $y = {}^1/_4$ (not shown) is closely similar because of the pseudotetragonal symmetry. Attempts to refine individual positions for C(1)–C(6) and N(1) of the first molecule and of C(7)–C(12) and N(2) of the second molecule failed because of strong correlations in the least-squares matrix. Refinements using idealized rigid molecules were successful, and the key concern is the degree to which the final answer depends on the strict implication from the observed diffraction data rather than from the computer modeling.

**Table I.** Crystallographic Data for MAPO-43

| | |
|---|---|
| formula | $(Mg_{2.2}Al_{5.8})(P_8O_{32})\cdot 2.2(C_3H_7)_2NH_2$ |
| crystal shape; size, mm | square bipyramid; axes 0.10, 0.10, 0.06 |
| space group | $I112/b$ |
| X-ray source, λ Å | Rigaku rotating anode at 55 kV 200 ma, Cu-target, 1.5418 |
| monochromator | graphite |
| cell dimensions | |
| *a*, Å | 10.2192 (2) |
| *b*, Å | 10.2198 (3) |
| *c*, Å | 10.0126 (3) |
| γ, deg | 90.987 (2) |
| volume, Å$^3$ | 1045.55 (4) |
| density calc, g/cm$^3$ | 1.897 |
| temperature | room temperature |
| diffractometer | Picker, Crystal Logic Automation |
| scan technique | $\theta$–$2\theta$ |
| speed, deg/min | 1.5 |
| range, deg | 1.8–2.4 |
| background | from peak profile analysis |
| total intensities | 1813 |
| merge *R* | 0.02 |
| unique data set | 854 |
| sin $\theta/\lambda_{max}$ | 0.58 |
| absorption correction | yes, analytical method[9] |
| transmission factors | 0.775–0.803 |
| $\mu$, cm$^{-1}$ | 56.8 |

The assumption of the two geometrically congruent molecules with a planar zigzag $C_3NC_3$ backbone (N–C = 1.479 Å; C–C = 1.541 Å; C–H and N–H = 0.95 Å; all angles = 109.5 Å) led to a stable least-squares solution with a plausible fit to the electron density (Figure 2a). Note that each molecule has images because it is asymmetrical with respect to the 2-fold symmetry axes and inversion centers. This asymmetry results from the hydrogen bonding of N to framework oxygens (see Discussion). The difference-Fourier synthesis (Figure 2b) showed that about five-sixths of the electron density had been accounted for. It appeared that each molecule might be slightly nonplanar, but a least-squares refinement allowing the molecule to undergo torsional rotations about C–C and C–N bonds while fixing the shape of the C and N tetrahedra did not improve the fit. A second refinement allowing these torsional movements plus adjustment of the C–C, C–N bond lengths and the tetrahedral angles also failed to produce any significant improvement.

In the final model, 78 variables were refined: scale factor, isotropic extinction parameter, atomic positions, anisotropic displacement factors

(8) Bennett, J. M.; Cohen, J. P.; Flanigen, E. M.; Pluth, J. J.; Smith, J. V. *Am. Chem. Soc. Symp. Ser.* **1983**, *218*, 109.
(9) Sheldrick, G. M. Computer program. Cambridge University, England.

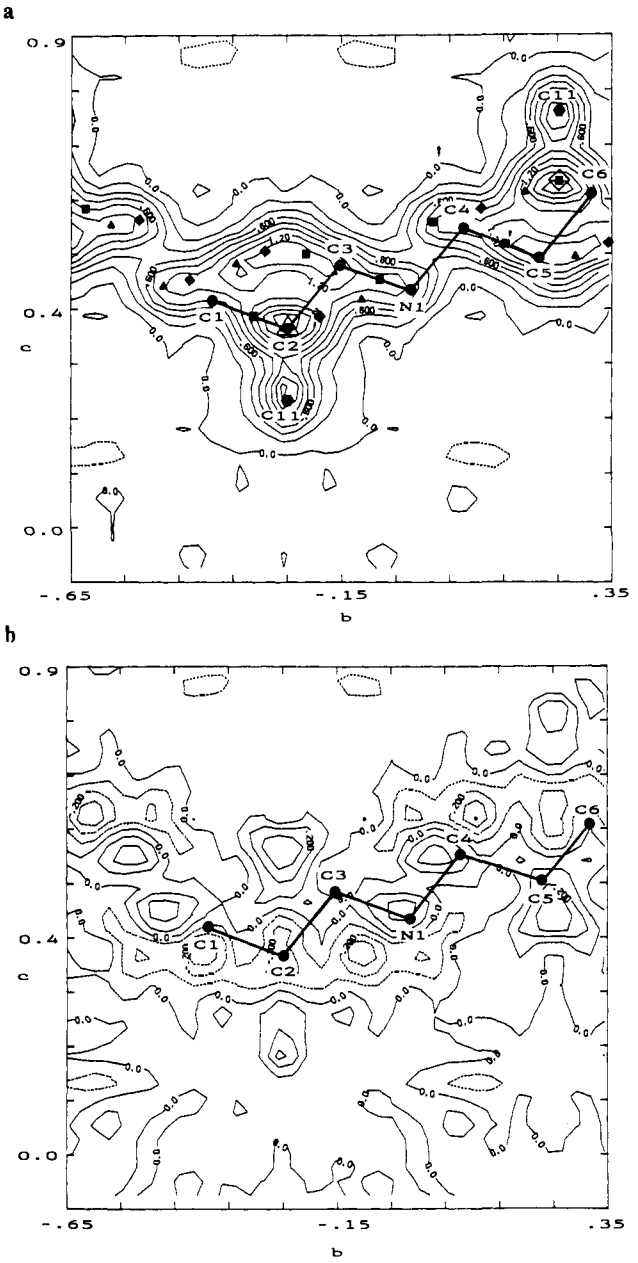


**Figure 2.** (a, top) Electron density at $x = 0$ after subtraction of the framework atoms. The large filled circles joined by heavy lines show the position of an idealized planar molecule C(1)–C(6),N(1) resulting from least-squares fitting. Triangles show the positions for a molecule related by the 2-fold axis at $y = \pm 1/4$. Diamonds and squares show the positions for molecules related by centers of symmetry at 0, 0, $1/2$ and 0, $-1/2$, $1/2$. Hexagons show the projection of C(11) from the second type of molecule C(7)–C(12),N(2) that lies near the $x = 0$ plane. The C(8) atom nearly superimposes upon C(2) and is not shown separately. (b, bottom) Corresponding difference-Fourier synthesis with contour interval halved. The highest positive density in (b) corresponds to about one-sixth of the highest in (a). Only one molecule is shown.

for framework atoms, isotropic ones for C, N, and H group atoms, individual occupancy factors for Al and P, and an overall occupancy factor for each group. Where the electron density of group atoms overlapped, the isotropic temperature factors were equated to improve the convergence of the refinement: N(1),C(4),C(1); C(2),C(6); C(3),C(5); N(2),C(10),C(7); C(8),C(12); C(9),C(11). The isotropic temperature factors of the hydrogen atoms were set to the same value as the atom to which they were attached and neutral scattering factors[10] were used. The population factors of both P and Al,Mg refined to a value significantly less than 1 because X-ray scattering factors depend on the state of ionization and the assumption of neutral scattering atoms is not totally correct. The smaller population factor for the Al positions [0.901 (4)] than for the P positions [0.922 (4)] is consistent with the expectation from the chemical analysis that 28% of the Al sites are occupied by Mg. The population factors of the two template molecules refined to 1.06 (2) and 1.10 (2) for the molecules containing N(1) and N(2), respectively. These values are consistent with the assumption that a charged template molecule (di-*n*-propylammonium ion) is present in the channels for each Mg incorporated into the framework.

Estimated errors in intensity calculated by $\sigma_I = P[S + t^2B + k^2(S + tB)^2]^{1/2}$, where $P$ = scan rate, $S$ = peak scan count, $B$ = total background count, $k$ = instability constant, and $t$ = ratio of peak to background observation times, were converted to $\sigma_F$ by correcting for Lorentz and polarization effects assuming the monochromator crystal was half-perfect and half-mosaic. The final least-squares refinement minimized differences in $F$'s, $w = \sigma_F^{-2}$, $R = 0.038$, $wR = 0.049$, $S = 4.0$; maximum shift/e.s.d. = 0.002; maximum and minimum heights on final difference-Fourier map are 0.4 and −0.4 eÅ$^{-3}$; computer programs—local data reduction, SHELX76,[9] ORFFE,[11] ORTEP,[12] AGNOST.[13] Final atomic coor-

**Table II.** Atomic Positions and Displacements of MAPO-43

| atom | $x$ | $y$ | $z$ | $U_{eq}$[a] |
|---|---|---|---|---|
| P | 0.34269 (7) | 0.09267 (6) | 0.37490 (7) | 0.0218 (3) |
| Al | 0.14938 (8) | 0.10057 (8) | 0.12505 (8) | 0.0223 (3) |
| O(1) | 0.1756 (2) | 0.2667 (2) | 0.0794 (2) | 0.0425 (7) |
| O(2) | 0.4833 (2) | 0.0742 (2) | 0.3297 (2) | 0.0427 (8) |
| O(3) | 0.2514 (2) | 0.0604 (2) | 0.2608 (2) | 0.0516 (8) |
| O(4) | 0.3101 (2) | 0.0016 (2) | 0.4896 (2) | 0.0516 (8) |
| N(1) | 0.001 (3) | −0.018 (1) | 0.434 (2) | 0.14 (1) |
| H(1) | −0.077 (3) | −0.007 (1) | 0.384 (2) | 0.14 (1) |
| H(2) | 0.075 (3) | −0.001 (1) | 0.378 (2) | 0.14 (1) |
| C(1) | 0.009 (3) | −0.391 (1) | 0.418 (2) | 0.14 (1) |
| H(3) | 0.007 (3) | −0.451 (1) | 0.345 (2) | 0.14 (1) |
| H(4) | −0.065 (3) | −0.408 (1) | 0.474 (2) | 0.14 (1) |
| H(5) | 0.087 (3) | −0.402 (1) | 0.469 (2) | 0.14 (1) |
| C(2) | 0.004 (3) | −0.250 (1) | 0.366 (2) | 0.13 (2) |
| H(6) | 0.078 (3) | −0.233 (1) | 0.310 (2) | 0.13 (2) |
| H(7) | −0.074 (3) | −0.239 (1) | 0.366 (2) | 0.13 (2) |
| C(3) | 0.006 (3) | −0.154 (1) | 0.484 (2) | 0.041 (4) |
| H(8) | 0.084 (3) | −0.165 (1) | 0.534 (2) | 0.041 (4) |
| H(9) | −0.068 (3) | −0.170 (1) | 0.540 (2) | 0.041 (4) |
| C(4) | 0.004 (3) | 0.075 (1) | 0.547 (2) | 0.14 (1) |
| H(10) | −0.070 (3) | 0.058 (1) | 0.603 (2) | 0.14 (1) |
| H(11) | 0.082 (3) | 0.063 (1) | 0.597 (2) | 0.14 (1) |
| C(5) | −0.001 (3) | 0.216 (1) | 0.495 (2) | 0.041 (4) |
| H(12) | 0.073 (3) | 0.233 (1) | 0.439 (2) | 0.041 (4) |
| H(13) | −0.079 (3) | 0.227 (1) | 0.445 (2) | 0.041 (4) |
| C(6) | 0.001 (3) | 0.312 (1) | 0.613 (2) | 0.13 (2) |
| H(14) | −0.002 (3) | 0.400 (1) | 0.581 (2) | 0.13 (2) |
| H(15) | 0.079 (3) | 0.301 (1) | 0.663 (2) | 0.13 (2) |
| H(16) | −0.073 (3) | 0.295 (1) | 0.669 (2) | 0.13 (2) |
| N(2) | 0.232 (1) | 0.754 (3) | 0.319 (2) | 0.14 (1) |
| H(17) | 0.246 (1) | 0.679 (3) | 0.373 (2) | 0.14 (1) |
| H(18) | 0.247 (1) | 0.831 (3) | 0.370 (2) | 0.14 (1) |
| C(7) | −0.141 (1) | 0.765 (3) | 0.332 (2) | 0.14 (1) |
| H(19) | −0.200 (1) | 0.771 (3) | 0.405 (2) | 0.14 (1) |
| H(20) | −0.160 (1) | 0.689 (3) | 0.282 (2) | 0.14 (1) |
| H(21) | −0.150 (1) | 0.840 (3) | 0.277 (2) | 0.14 (1) |
| C(8) | 0.000 (1) | 0.760 (3) | 0.386 (2) | 0.16 (2) |
| H(22) | 0.009 (1) | 0.685 (3) | 0.441 (2) | 0.16 (2) |
| H(23) | 0.019 (1) | 0.837 (3) | 0.436 (2) | 0.16 (2) |
| C(9) | 0.097 (1) | 0.752 (3) | 0.268 (2) | 0.039 (4) |
| H(24) | 0.085 (1) | 0.824 (3) | 0.210 (2) | 0.039 (4) |
| H(25) | 0.081 (1) | 0.672 (3) | 0.220 (2) | 0.039 (4) |
| C(10) | 0.325 (1) | 0.754 (3) | 0.205 (2) | 0.14 (1) |
| H(26) | 0.307 (1) | 0.679 (3) | 0.150 (2) | 0.14 (1) |
| H(27) | 0.315 (1) | 0.831 (3) | 0.154 (2) | 0.14 (1) |
| C(11) | 0.466 (1) | 0.748 (3) | 0.258 (2) | 0.039 (4) |
| H(28) | 0.482 (1) | 0.819 (3) | 0.317 (2) | 0.039 (4) |
| H(29) | 0.478 (1) | 0.668 (3) | 0.304 (2) | 0.039 (4) |
| C(12) | 0.563 (1) | 0.756 (3) | 0.140 (2) | 0.16 (2) |
| H(30) | 0.650 (1) | 0.753 (3) | 0.173 (2) | 0.16 (2) |
| H(31) | 0.551 (1) | 0.836 (3) | 0.094 (2) | 0.16 (2) |
| H(32) | 0.547 (1) | 0.685 (3) | 0.081 (2) | 0.16 (2) |

[a] $U_{eq}$ is defined as $1/3\sum_{i=1}^{3}\sum_{j=1}^{3}U_{ij}a_i^*a_j^*(\mathbf{a}_i\cdot\mathbf{a}_j)$.

(10) *International Tables for X-ray Crystallography*; Kynoch Press: Birmingham, 1974; Vol. IV, pp 72–98.

(11) Busing, W. R.; Martin, K.; Levy, H. A. Report ORNL-TM-306. Oak Ridge National Laboratory, TN, 1964.

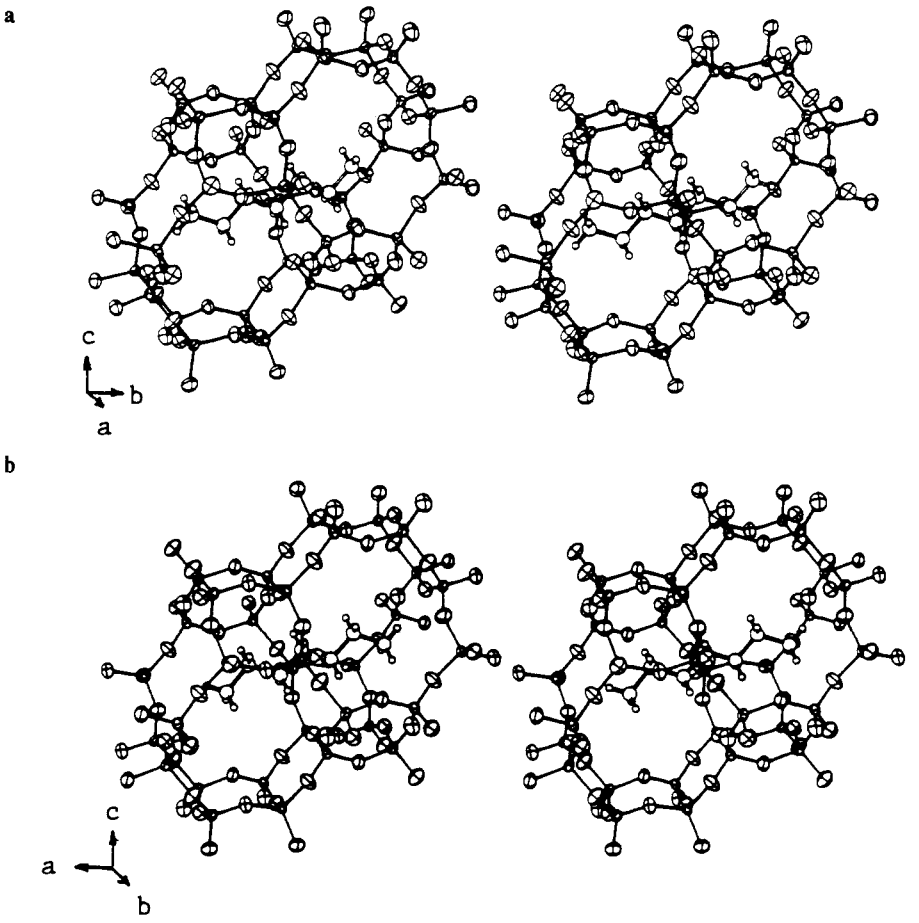


**Figure 3.** Stereoviews of the framework around the two types of template molecules. Displacement ellipsoids for the framework atoms are shown at the 50% probability level and the spheres for the template atoms are arbitrary.

dinates and displacement factors are given in Table II, and interatomic distances (with and without riding motion) and angles in Tables III and IV. A table of anisotropic thermal parameters (Table V) and a listing of observed and calculated structure factors are available as supplementary material.

## Discussion

**Framework Topology.** MAPO-43 has the same topological type of 3-D framework as the zeolite gismondine (Figure 1). Whereas gismondine has Si and Al alternating on tetrahedral nodes MAPO-43 has Al, Mg, and P. The GIS topology was first obtained during an enumeration[14] of 4-connected frameworks with parallel 4- and 8-membered rings.[15] The structure determination of gismondine[16,17] revealed alternation of Al and Si in the framework, but the deviation from tetragonal symmetry is somewhat different from that for MAPO-43. Because of the pseudosymmetry, it is possible to choose axes in more than one way. The present choice of a nonstandard space group matches that for gismondine in standard compilations of zeolite structures.[18,19]

The linkage of $4.8^2$ 3-connected 2D nets to form the double-crankshaft chains along both the *a* and *b* axes of the gismondine framework is described in a recent review.[20] Channels bounded by 8-rings (Figure 1) run parallel to the *a* and *b* axes at levels differing by $c/4$ in accord with the $4_1$ screw axis parallel to *c* in the neutral ideal framework. These channels intersect to generate a 3D channel system.

**Table III.** MAPO-43 Framework: Interatomic Distances (Å) and Angles (deg)

| | centroid | riding[a] | | |
|---|---|---|---|---|
| P-O(1) | 1.523 (2) | 1.540 (2) | O(1)-P-O(2) | 109.7 (1) |
| P-O(2) | 1.522 (2) | 1.540 (2) | O(1)-P-O(3) | 110.4 (1) |
| P-O(3) | 1.508 (3) | 1.535 (3) | O(1)-P-O(4) | 108.9 (1) |
| P-O(4) | 1.512 (3) | 1.539 (3) | O(2)-P-O(3) | 109.2 (1) |
| mean | 1.516 | 1.539 | O(2)-P-O(4) | 110.4 (1) |
| | | | O(3)-P-O(4) | 108.1 (1) |
| Al-O(1) | 1.775 (2) | 1.789 (2) | O(1)-Al-O(2) | 109.8 (1) |
| Al-O(2) | 1.773 (2) | 1.787 (2) | O(1)-Al-O(3) | 109.9 (1) |
| Al-O(3) | 1.766 (3) | 1.787 (3) | O(1)-Al-O(4) | 109.6 (1) |
| Al-O(4) | 1.765 (3) | 1.787 (3) | O(2)-Al-O(3) | 109.6 (1) |
| mean | 1.770 | 1.787 | O(2)-Al-O(4) | 109.9 (1) |
| | | | O(3)-Al-O(4) | 108.0 (1) |
| P-O(1)-Al | 143.8 (2) | | P-O(3)-Al | 153.9 (2) |
| P-O(2)-Al | 144.0 (2) | | P-O(4)-Al | 153.7 (2) |

[a] Oxygen riding on tetrahedral atom.

**Location of Mg and Framework Ordering.** All the analytical and crystallographic data are consistent with random incorporation of Mg in the Al site. Within experimental uncertainty, (Al + Mg) = P (see previous discussion). Crystal-chemically, tetrahedral Mg is closer to Al than P from the viewpoint of both ionic charge and size. All the electron density in the channels, and essentially all of the pore volume, can be accounted for by the encapsulated species. The consistently small values of $U_{eq}$ for the framework atoms (Table II) rule out any significant deviation from tetrahedral

(12) Johnson, C. K. Report ORNL-3794. Oak Ridge National Laboratory, TN, 1965.
(13) Ibers, J. Personal Communication.
(14) Smith, J. V.; Rinaldi, F. *Mineral. Mag.* **1962**, *33*, 202.
(15) Smith, J. V. *Am. Mineral.* **1978**, *63*, 960.
(16) Fisher, K. F. *Am. Mineral.* **1963**, *48*, 664.
(17) Fischer, K. F.; Schramm, V. *Am. Chem. Soc., Adv. Chem. Ser.* **1971**, *101*, 250.
(18) Meier, W. M.; Olson, D. H. *Am. Chem. Soc. Adv. Chem. Ser.* **1971**, *101*, 155.
(19) Meier, W. M.; Olson, D. H. *Atlas of Zeolite Structure Types*; International Zeolite Association, 1978.
(20) Smith, J. V. *Chem. Rev.* **1988**, *88*, 149.

**Table IV.** MAPO-43 Interatomic Distances (Å) and Angles (deg) Involving C and N Atoms of Template Molecule

| Intramolecular: | | Refined as Planar Rigid Group | |
|---|---|---|---|
| all N-C | 1.479 | all C-C-C | 109.5 |
| all C-C | 1.541 | all C-N-C | 109.5 |
| all C-H | 0.950 | all C-C-N | 109.5 |
| all N-H | 0.950 | all C-C-H | 109.5 |
| | | all N-C-H | 109.5 |
| | | all C-N-H | 109.5 |
| | | all H-C-H | 109.5 |
| | | all H-N-H | 109.5 |

Nitrogen-Oxygen, Hydrogen-Oxygen Close Approaches, Possible Hydrogen Bonds

| | | | |
|---|---|---|---|
| N(1)-O(2) | 2.81 (2) | C(3)-N(1)-O(2) | 130 (1) |
| N(1)-O(3) | 3.18 (3) | C(3)-N(1)-O(3) | 113 (2) |
| N(1)-O(4) | 3.21 (3) | C(3)-N(1)-O(3) | 118 (2) |
| N(1)-O(4) | 3.28 (3) | C(4)-N(1)-O(2) | 121 (1) |
| N(1)-O(3) | 3.32 (3) | C(4)-N(1)-O(3) | 105 (1) |
| H(1)-O(2) | 2.37 (2) | C(4)-N(1)-O(3) | 108 (2) |
| H(1)-O(3) | 2.39 (2) | O(3)-N(1)-O(3) | 104 (1) |
| H(1)-O(4) | 2.70 (3) | N(1)-H(1)-O(2) | 108 (2) |
| H(2)-O(3) | 2.23 (3) | N(1)-H(1)-O(3) | 168 (2) |
| H(2)-O(2) | 2.41 (2) | N(1)-H(1)-O(4) | 120 (2) |
| H(2)-O(4) | 2.65 (3) | N(1)-H(2)-O(2) | 105 (2) |
| | | N(1)-H(2)-O(3) | 173 (1) |
| | | N(1)-H(2)-O(4) | 118 (2) |
| N(2)-O(1) | 2.79 (2) | C(9)-N(2)-O(1) | 130 (1) |
| N(2)-O(4) | 3.15 (3) | C(9)-N(2)-O(4) | 115 (2) |
| N(2)-O(3) | 3.19 (3) | C(9)-N(2)-O(4) | 115 (2) |
| N(2)-O(3) | 3.31 (3) | C(10)-N(2)-O(1) | 120 (1) |
| N(2)-O(4) | 3.32 (3) | C(10)-N(2)-O(4) | 106 (2) |
| H(17)-O(1) | 2.29 (2) | C(10)-N(2)-O(4) | 106 (2) |
| H(17)-O(4) | 2.38 (2) | O(4)-N(2)-O(4) | 104 (1) |
| H(17)-O(3) | 2.79 (3) | N(2)-H(17)-O(1) | 112 (2) |
| H(18)-O(4) | 2.20 (3) | N(2)-H(17)-O(4) | 172 (2) |
| H(18)-O(1) | 2.46 (2) | N(2)-H(17)-O(3) | 116 (2) |
| H(18)-O(3) | 2.59 (3) | N(2)-H(18)-O(1) | 100 (2) |
| | | N(2)-H(18)-O(4) | 172 (2) |
| | | N(2)-H(18)-O(3) | 121 (2) |

Carbon-Oxygen Close Approaches, Possible Hydrogen Bonds

| | | | |
|---|---|---|---|
| C(1)-O(2) | 3.11 (2) | C(7)-O(1) | 3.11 (2) |
| C(1)-O(4) | 3.41 (3) | C(7)-O(3) | 3.36 (3) |
| C(3)-O(4) | 3.46 (3) | C(7)-O(4) | 3.46 (2) |
| C(4)-O(2) | 3.21 (2) | C(10)-O(1) | 3.23 (2) |
| C(4)-O(4) | 3.28 (3) | C(10)-O(3) | 3.28 (3) |
| C(4)-O(4) | 3.31 (3) | C(10)-O(3) | 3.31 (3) |
| C(5)-O(1) | 3.41 (3) | C(11)-O(2) | 3.42 (3) |
| C(5)-O(1) | 3.43 (3) | C(11)-O(2) | 3.42 (3) |
| C(6)-O(2) | 3.45 (2) | C(12)-O(1) | 3.47 (2) |

Shortest Distance between Carbon Atoms of Adjacent Molecules

| | | | |
|---|---|---|---|
| C(1)-C(6) | 3.60 (3) | C(7)-C(12) | 3.59 (3) |
| C(1)-C(12) | 4.27 (3) | C(7)-C(6) | 4.30 (3) |
| C(1)-C(11) | 5.03 (3) | C(7)-C(5) | 5.01 (3) |
| C(6)-C(8) | 5.11 (3) | C(12)-C(2) | 5.04 (3) |

coordination. Both the (Al,Mg) and P tetrahedra are nearly regular (Table III), and the P-O and Al,Mg-O distances are consistent with those in other framework structures after adjustment for riding motion. In particular, the mean value of 1.787 Å of Al,Mg-O is consistent with the composition $(Al_{0.72}Mg_{0.28})$ deduced from electron microprobe analysis, when the fact that $Mg^{2+}$ has a larger ionic radius than Al is taken into account.

**Location of the Di-*n*-propylamine Species.** Ignoring details of the exact shape of the encapsulated species, Figure 3 (a and b) shows how the two types of species lie in the channels. The key feature is the close approach of each N atom to three framework oxygens of an 8-ring (Figure 4, a and b). This close approach is consistent with hydrogen bonding, but unfortunately this cannot be tested directly from the diffraction evidence because the inferred protons do not scatter with sufficient strength. The simplest chemical interpretation is that each addition of a proton to an NH

(21) Shannon, R. D. *Acta Crystallogr.* **1976**, *A32*, 751.

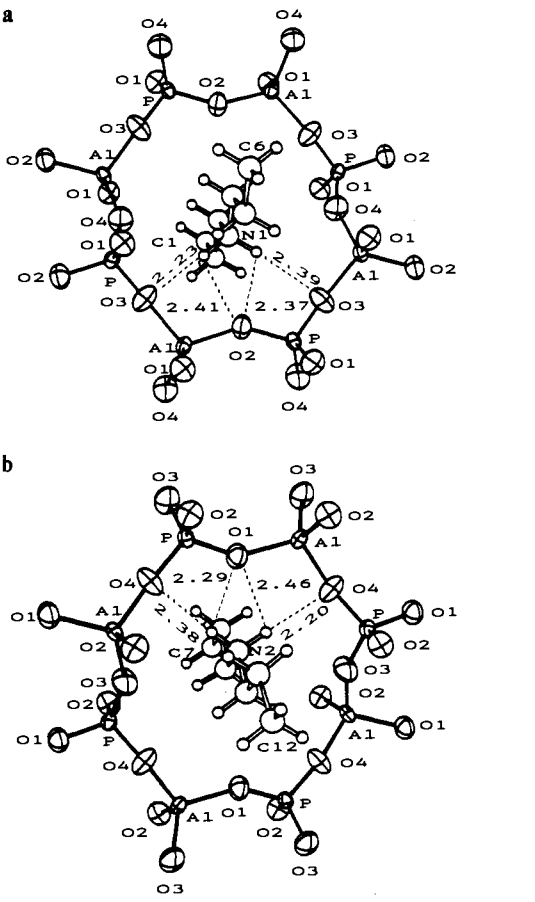


**Figure 4.** Proposed hydrogen bonding from $NH_2$ (dashed lines) of the ionized organic species to framework oxygens of the 8-rings. Observed displacement ellipsoids for the framework atoms are shown at the 50% probability level. Spheres for the atoms of the template molecule are arbitrary.

to produce $NH_2^+$ is compensated by incorporation of one Mg in an Al site. The pair of protons are then assumed to project toward the three oxygen atoms in approximately the positions shown in Figure 4.

**Location and Packing of the Di-*n*-propylamine Species.** The two perpendicular $4.8^2$ nets form a network of intersecting 2-dimensional straight channels in the *a,b* plane (Figure 1). Movement through the channels parallel to *c* is accomplished by a zigzag path. Each di-*n*-propylammonium species lies nearly parallel to either the *a* or *b* axis (the structure is pseudotetragonal) and extends into and blocks two channels intersecting at right angles (Figure 1). The (Al,Mg) and P alternation enforces monoclinic symmetry and automatically requires that there are two crystallographically different types of molecules. However, the two types obey the pseudotetragonal symmetry of the ideal neutral framework within about 0.2 Å. It is important to recognize that the inferred hydrogen bonding from the $NH_2$ unit at the center of each molecule forces the molecule to disobey the symmetry of the monoclinic space group of the ordered framework. Thus C(2) in Figure 2a lies approximately on a 2-fold rotation axis which is disobeyed by all other atoms in the molecule. Hence there must be a statistical averaging of two positions shown by dots and triangles. Similarly there is statistical averaging of positions related by a center of symmetry. In total, there are $2 \times 2 = 4$ positions, but there is only one type of chemical bonding between a molecule and the framework. It is also important to recognize that hydrogen bonding is not possible for a molecule positioned to obey a 2-fold rotation axis. Because there is overlap of positions from the eight possible locations of molecules (Figure 2), it is not possible to obtain a least-squares solution to the individual atomic positions. Use of a constrained geometry resulted in a solution, but it is quite certain that there are uncertainties

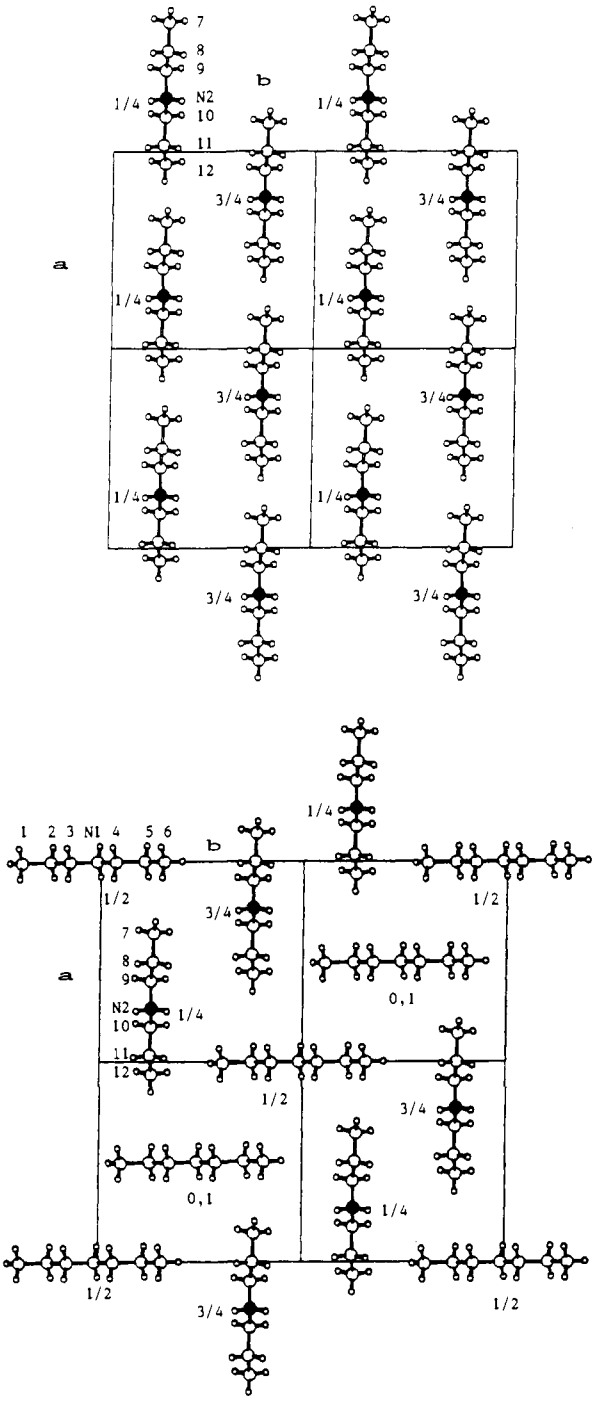


**Figure 5.** Two ordered ways of packing the organic species: (a) parallel and (b) herringbone. Four unit cells are shown for each pattern. Approximate heights are given as a fraction of *c* repeat.

in the individual atomic positions that amount to several tenths of an Ångström unit.

How do adjacent molecules fit together? The most obvious solution is to pack the molecules in a simple parallel array in each plane perpendicular to *c* (Figure 5a). Another simple solution is to alternate the molecular orientations to generate a herringbone pattern (Figure 5b). From the viewpoint of van der Waals bonding between the end C atoms of adjacent molecules, the herringbone pattern generates only one set of distances near 4.3 Å whereas the parallel pattern yields two sets of distances near 3.6 and 5.0 Å (Table IV). In silicalite[22,23] the end C atoms of the tetrapropylammonium species lie at 3.6–3.8 Å. Because van der Waals bonding is so weak in relation to ionic and covalent bonding, there can be little difference in Gibbs free energy between ideal parallel and herringbone arrays. Because the two types of ideal arrays are topologically incompatible, it seems likely that domains occur with complex boundary regions.

How many molecules can occur on average in a unit cell? Both of the ideal parallel and herringbone arrays generate exactly 2 molecules per cell. It is not clear what might happen in a boundary region between domains. In principle, it may be possible to invent complex arrays in which the molecules are squeezed together so that their end C atoms are all at 3.6–3.8 Å rather than at the 4.3 or 3.6/5.0 Å distances of the ideal arrays. On the other hand, there might be vacancies that reduce the number below 2. Although the refinement yielded 2.16 (4) N atoms per cell, it is necessary to be cautious in accepting population refinements of disordered structures at face value. If there are really only two molecules per cell, there are too many Mg atoms (2.2) for charge balance. Again it is necessary to be cautious because the theory of matrix corrections for electron microprobe analysis of samples with light elements of similar atomic number is rather uncertain. If there is really a small excess of Mg over N, it can be compensated readily by incorporation of hydroxyl.

## Conclusions and Implications for Crystallization Processes

The present data on MAPO-43 are consistent with a disordered packing of approximately two organic species per monoclinic cell in a gismondine-type pseudotetragonal framework with alternation of 8 P and approximately 6 Al + 2 Mg. The interatomic distances are consistent with ionization of the original di-*n*-propylamine so that each central ammonium functional group can form bifurcated hydrogen bonds to three oxygen atoms of an 8-ring. This bonding enforces an off-centered position of each organic ion which violates the formal crystallographic symmetry of the framework. Positional disorder and probably domain structure allows statistical obeyance of the framework symmetry. This disorder has important implications for the structure-directing role of the organic species during crystallization from a gel.

The structural, synthetic, and physicochemical concepts pertinent to aluminophosphate-based molecular sieves have been reviewed.[24] These concepts are related to ones developed for the role of templates in the synthesis of aluminosilicate molecular sieves (zeolites).[25-28] In general for the aluminophosphate-based molecular sieves, "the structure-directing role of the template is dominated by stereospecific space-filling and stoichiometry between the template and the framework, and is influenced to a lesser extent by framework charge compensation."[24]

Specifically for MAPO-43, it appears that during the incubation period of the gel each molecule becomes ionized and one Mg atom per molecule takes up a neighboring position in the protoframework. The framework topology is controlled by complex geometrical factors related to ionic and van der Waals bonding. Only part of the gel in the present synthesis is transformed into a gismondine topology, and other fractions yield MAPO-46 and MAPO-11 topologies. Because the final crystalline product of MAPO-43 has molecular disorder, each crystal must incorporate pieces of protoframework with molecules lying in different orientations. A detailed review of the current status of crystallographic data on the inorganic–organic relationships in aluminophosphate-based molecular sieves is being prepared.

To conclude, the present crystallographic study raises questions on the kinetics and stereospecificity of the crystallization of aluminophosphate–organic gels that will require many further

(22) Price, G. D.; Pluth, J. J.; Smith, J. V.; Bennett, J. M.; Patton, R. L. *J. Am. Chem. Soc.* **1982**, *104*, 5971.
(23) von Koningsveld, H.; van Bekkum, H.; Jansen, J. C. *Acta Crystallogr. B* **1987**, *43*, 127.
(24) Flanigen, E. M.; Patton, R. L.; Wilson, S. T. In *Innovation in Zeolite Materials Science*; Grobet, P. J., Mortier, W. J., Vansant, E. F., Schulz-Ekloff, G., Eds.; Elsevier: Amsterdam; p 13.
(25) Lok, B. M.; Cannan, T. R.; Messina, C. A. *Zeolites* **1983**, *3*, 282.
(26) Gabelica, Z.; Derouane, E. G.; Blom, N. *Am. Chem. Soc. Symp. Ser.* **1984**, *248*, 219.
(27) Iton, L.; Brun, T.; White, J. W. *Ann. Rep. Intense Pulsed Neutron Source*; Argonne National Laboratory, 1983; p 34.
(28) White, J. W. *Trans. Am. Cryst. Assoc.* **1987**, *23*, 1.

studies with use of scattering, spectroscopic, and resonance techniques. Ultimately the combined studies should throw light on crystallization processes in general, including ones involving biological materials.

**Acknowledgment.** We thank S. T. Wilson, R. L. Patton, R. L. Bedard, and E. M. Flanigen for discussion of the results, I. M. Steele for electron microprobe analysis, and N. Weber for manuscript preparation. Financial support was provided by NSF Grants CHE-8618041 and DMR-8519460 (Materials Research Laboratory) and by Union Carbide Corp.

**Supplementary Material Available:** Table of anisotropic displacement parameters (Table IV) (1 page); listing of observed and calculated structure factors (5 pages). Ordering information is given on any current masthead page.

# Molecular Engineering of Solid-State Materials: Organometallic Building Blocks

**Paul J. Fagan,* Michael D. Ward,* and Joseph C. Calabrese**

*Contribution No. 4744 from the Central Research and Development Department, E. I. du Pont de Nemours & Company, Experimental Station, Wilmington, Delaware 19880-0328.*
*Received May 24, 1988*

**Abstract:** The syntheses of the reagents $[Cp^*Ru(CH_3CN)_3]^+(OTf^-)$ (**1**) ($Cp^* = \eta$-$C_5(CH_3)_5$; OTf = $CF_3SO_3$) and $[Cp^*Ru(\mu_3\text{-}Cl)]_4$ (**2**) are reported. Reaction of **1** with aromatic hydrocarbons that are used as geometric templates allows the preparation of polycationic complexes with particular shapes and geometries of positive charge. Using [2$_2$]-1,4-cyclophane, the cylindrical rod-like complexes $[(Cp^*Ru)_2(\eta^6,\eta^6\text{-}[2_2]\text{-}1,4\text{-cyclophane})]^{2+}(OTf^-)_2$, $[Cp^*Ru([2_2]\text{-}1,4\text{-cyclophane})CoCp^*]^{3+}(OTf^-)_3$, and $\{[Cp^*Ru(\eta^6,\eta^6\text{-}[2_2]\text{-}1,4\text{-cyclophane})]_2Ru\}^{4+}(OTf^-)_4$ have been synthesized. With triptycene as a template, a triangular trication isolated as the complex $[(Cp^*Ru)_3(\eta^6,\eta^6,\eta^6\text{-triptycene})]^{3+}(OTf^-)_3$ can be prepared. Reaction of **1** with tetraphenylmethane, -silane, -germane, -stannane, and -plumbane results in formation of tetrahedral tetracations isolated as the complexes $\{[Cp^*Ru(\eta\text{-}C_6H_5)]_4E\}^{4+}(OTf^-)_4$ (E = C, Si, Ge, Sn, Pb). The structure of $\{[Cp^*Ru(\eta\text{-}C_6H_5)]_4Ge\}^{4+}(OTf^-)_4$ has been determined by a single-crystal X-ray analysis (monoclinic-*b*, $P2_1/c$ (No. 14); $a$ = 22.633 (3) Å, $b$ = 12.826 (2) Å, $c$ = 24.944 (3) Å, $\beta$ = 93.49 (1)°, $V$ = 7227.6 Å$^3$, $Z$ = 4) and is compared to the structural parameters of the tetracations $\{[Cp^*Ru(\eta\text{-}C_6H_5)]_4E\}^{4+}$ (E = C, Si). Reaction of **1** with hexakis(*p*-methoxyphenoxy)benzene yields $\{[Cp^*Ru(p\text{-}CH_3O\text{-}\eta\text{-}C_6H_4\text{-}O)]_6C_6\}^{6+}(OTf^-)_6$. A single-crystal X-ray analysis of $\{[Cp^*Ru(p\text{-}CH_3O\text{-}\eta\text{-}C_6H_4\text{-}O)]_6C_6\}(OTf)_6\cdot 6CH_3NO_2$ (triclinic, $P\bar{1}$ (No. 2); $a$ = 15.784 (3) Å, $b$ = 16.539 (4) Å, $c$ = 17.817 (3) Å, $\alpha$ = 65.47 (2)°, $\beta$ = 61.82 (2)°, $\gamma$ = 63.86 (3)°, $V$ = 3552.2 Å$^3$, $Z$ = 1) shows that the hexacation contains an octahedral array of ruthenium atoms. With *p*-quaterphenyl and *p*-sexiphenyl, the reaction with **1** leads to formation of the tetracation $[(Cp^*Ru)_4(\eta^6,\eta^6,\eta^6,\eta^6\text{-}p\text{-quaterphenyl})]^{4+}(OTf^-)_4$ and hexacation $[(Cp^*Ru)_6(\eta^6,\eta^6,\eta^6,\eta^6,\eta^6,\eta^6\text{-}p\text{-sexiphenyl})]^{6+}(OTf^-)_6$, respectively. A single-crystal X-ray analysis of the complex $[(Cp^*Ru)_4(\eta^6,\eta^6,\eta^6,\eta^6\text{-}p\text{-quaterphenyl})](OTf)_4$ has been performed (triclinic, $P\bar{1}$ (No. 2); $a$ = 12.897 (3) Å, $b$ = 13.630 (2) Å, $c$ = 11.906 (2) Å, $\alpha$ = 108.31 (1)°, $\beta$ = 107.39 (2)°, $\gamma$ = 100.38 (1)°, $V$ = 1807.3 Å$^3$, $Z$ = 1). The potential use of these complexes for the rational control and preparation of solid-state molecular materials is discussed.

A fundamental problem in the synthesis of all solid-state materials is the difficulty associated with obtaining a desired three-dimensional arrangement of atoms or molecules. Finding methods to control predictably the arrangement of a crystalline material's constituents would greatly aid in the design of solids with desired physical properties. In this paper, we describe the synthesis, structure, and properties of organometallic building blocks with specific geometric shapes and arrangements of charge for the purpose of assembling molecular crystalline solids in a rational manner. In the following paper,[1] we show how these building blocks can be used in the construction of solid charge-transfer complexes.

The most commonly used approach to engineer a solid is to modify a previously determined structure type. For example, in traditional solid-state techniques, once a particular solid is synthesized empirically and its structure determined, the properties can be changed by substituting at a particular atom site with other ions of the appropriate size.[2] Other approaches also benefit from a predetermined lattice type as in the case of intercalation of molecules into layered solids[3] or into zeolite frameworks.[4] For

**Scheme I**

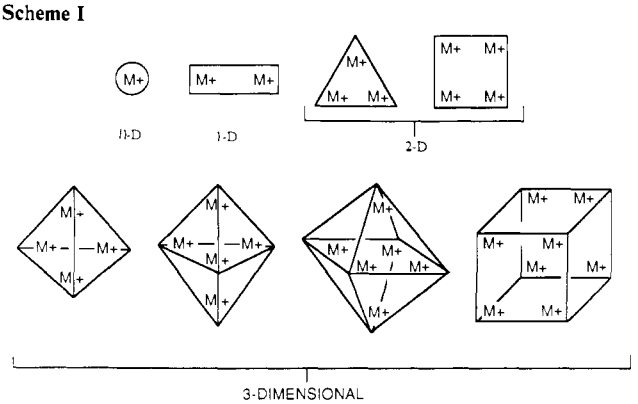


molecular crystalline solids, advantage can be taken of a pre-existing lattice network such as those utilized in the preparation

(1) Ward, M. D.; Fagan, P. J.; Calabrese, J. C.; Johnson, D. C. *J. Am. Chem. Soc.* **1988**, following paper in this journal.

(2) (a) Wells, A. F. *Structural Inorganic Chemistry*; Oxford University Press: Oxford, 1984. (b) West, A. R. *Solid State Chemistry and its Applications*; John Wiley & Sons: New York, 1984.

(3) (a) *Intercalation Layered Materials, NATO ASI Ser., Ser. B* **1986**, *148*. (b) Schöllhorn, R. *Inclusion Compd.* **1984**, *1*, 249-349. (c) *Intercalation Chemistry*; Whittingham, M. S., Jacobson, A. J., Eds.; Academic Press: New York, 1982.

(4) See for example: (a) Schowchow, F.; Puppe, L. *Angew. Chem.* **1975**, *87*, 659-667 and references therein. (b) Randas, S.; Thomas, J. M.; Betteridge, P. W.; Cheetham, A. K.; Davies, E. K. *Angew Chem.* **1984**, *96*, 629-637 and references therein.

0002-7863/89/1511-1698$01.50/0 